

# Frustrated minority spins in $\text{GeNi}_2\text{O}_4$

M. Matsuda<sup>1</sup>, J.-H. Chung<sup>2</sup>, S. Park<sup>3</sup>, T. J. Sato<sup>4</sup>, K. Matsuno<sup>5</sup>, H. Aruga Katori<sup>6,7</sup>, H. Takagi<sup>5,6,7</sup>,

K. Kakurai<sup>1</sup>, K. Kamazawa<sup>8</sup>, Y. Tsunoda<sup>9</sup>, I. Kagomiya<sup>9</sup>, C. L. Henley<sup>10</sup>, and S.-H. Lee<sup>8</sup>

<sup>1</sup>Quantum Beam Science Directorate, Japan Atomic Energy Agency, Tokai, Ibaraki 319-1195, Japan

<sup>2</sup>Department of Physics, Korea University, Seoul, Korea

<sup>3</sup>HANARO Center, Korea Atomic Energy Research Institute, Daejeon, Korea

<sup>4</sup>The Institute for Solid State Physics, University of Tokyo, Kashiwa, Chiba 277-8581, Japan

<sup>5</sup>Graduate School of Frontier Sciences, University of Tokyo, Kashiwa, Chiba 277-8561, Japan

<sup>6</sup>RIKEN (The Institute of Physical and Chemical Research), Wako, Saitama 351-0198, Japan

<sup>7</sup>CREST, Japan Science and Technology Corporation, Saitama 332-0012, Japan

<sup>8</sup>Department of Physics, University of Virginia, Charlottesville, Virginia 22904

<sup>9</sup>Department of Applied Physics, Waseda University,

3-4-1 Okubo, Shinjuku-ku, Tokyo 169-8555, Japan

<sup>10</sup>Department of Physics, Cornell University, Ithaca, NY 14853-2501

(Dated: November 6, 2018)

Recently, two consecutive phase transitions were observed, upon cooling, in an antiferromagnetic spinel  $\text{GeNi}_2\text{O}_4$  at  $T_{N1} = 12.1$  K and  $T_{N2} = 11.4$  K, respectively [1, 2]. Using unpolarized and polarized elastic neutron scattering we show that the two transitions are due to the existence of frustrated minority spins in this compound. Upon cooling, at  $T_{N1}$  the spins on the  $\langle 111 \rangle$  kagome planes order ferromagnetically in the plane and antiferromagnetically between the planes (phase I), leaving the spins on the  $\langle 111 \rangle$  triangular planes that separate the kagome planes frustrated and disordered. At the lower  $T_{N2}$ , the triangular spins also order in the  $\langle 111 \rangle$  plane (phase II). We also present a scenario involving exchange interactions that qualitatively explains the origin of the two purely magnetic phase transitions.

PACS numbers: 75.10.Jm, 75.25.+z, 75.50.Ee

In spinels  $\text{AB}_2\text{O}_4$ , the B sites form a highly frustrating network of corner-sharing tetrahedra, sometimes called a pyrochlore lattice.[3, 4] In the limit of only nearest-neighbor antiferromagnetic, isotropic exchange interactions, this system has macroscopic classical ground state degeneracy, leading to a spin liquid state down to zero temperature[5, 6, 8], or to ordering at unobservably low temperature [7]. The ground state degeneracy can however be lifted when the spin is coupled with lattice or orbital degrees of freedom. For instance, a spin-lattice coupling can induce a phase transition where a magnetic ordering and a lattice distortion occur simultaneously.[9, 10, 11] When an orbital degeneracy is present, a Jahn-Teller distortion usually occurs first upon cooling to lift the orbital degeneracy. If the resulting magnetic interactions are three dimensional, then a magnetic ordering occurs simultaneously. On the other hand, if the effective magnetic interactions in the distorted phase become low dimensional, the magnetic ordering is suppressed and may occur at a lower temperature, yielding two successive phase transitions.[12, 13, 14] Thus, it was surprising when  $\text{GeNi}_2\text{O}_4$  exhibited two successive phase transitions in despite of the absence of an orbital degeneracy of  $\text{Ni}^{2+}$  ( $3d^8$ ) ions.[1, 2] No structural distortion was observed by synchrotron X-ray or by neutron scattering measurements, indicating that the transitions are purely magnetic [2].

When viewed along the  $\langle 111 \rangle$  direction, the pyrochlore lattice can be described as alternating layers of a kagome

(of corner-sharing triangles) and a triangular lattice (with  $1/3$  as many spins per layer as the kagome layer). We have performed polarized and unpolarized elastic neutron scattering measurements on a single crystal of  $\text{GeNi}_2\text{O}_4$  to understand the nature of the phase transitions. Our results show that upon cooling, at  $T_{N1}$  the kagome (majority) spins order ferromagnetically in the  $\langle 111 \rangle$  plane and antiferromagnetically between the planes (phase I). Our polarized elastic neutron scattering indicates that the kagome spins are aligned along a high symmetry direction in the kagome plane. The antiferromagnetic stacking of the kagome planes induces zero internal magnetic field at the triangular spins that lie between the kagome planes and leaves the triangular spins frustrated. The triangular spins order in the  $\langle 111 \rangle$  plane only at the lower  $T_{N2} = 11.4$  K. In order to understand the experimental findings, we have considered a spin Hamiltonian with superexchange interactions among  $\text{Ni}^{2+}$  ions up to the fourth nearest neighbors. The model shows that dominant ferromagnetic  $J_1$  and antiferromagnetic  $J_4$  are the key interactions driving the first phase transition at  $T_{N1}$ , which is consistent with the Goodenough-Kanamori rules. However, it calls for ferromagnetic  $J_3$  and antiferromagnetic  $J'_3$  to describe the triangular layer behavior, which does not seem to obey the rules.

A single crystal of  $\text{GeNi}_2\text{O}_4$  was grown by chemical vapor transport method using  $\text{TeCl}_4$  as a transport agent. The crystal has the shape of an octahedron, an edge of which is typically about 1 mm long. Details of the sample

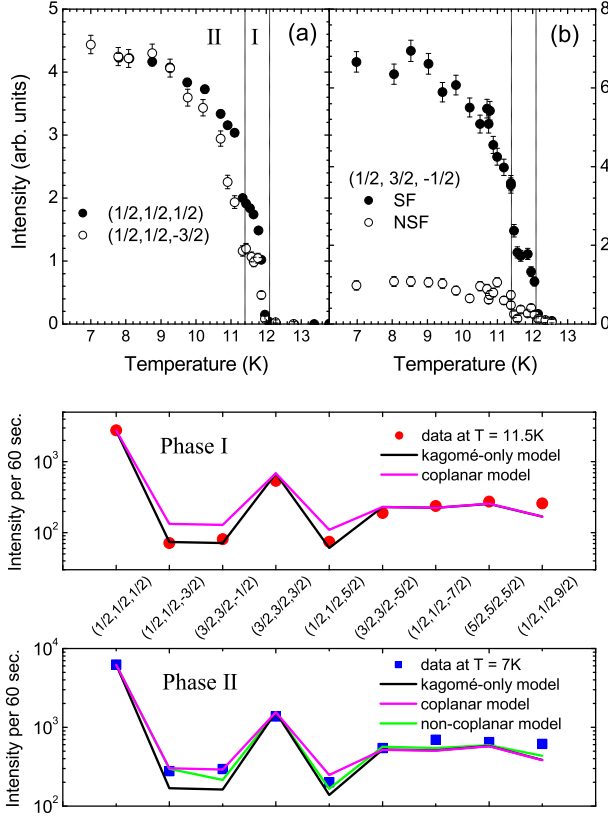


FIG. 1: Temperature dependence of the peak intensity of the  $(\frac{1}{2}, \frac{1}{2}, \frac{1}{2})$  and  $(\frac{1}{2}, \frac{1}{2}, \frac{3}{2})$  magnetic Bragg reflections measured with unpolarized neutrons (a), and that of the  $(\frac{1}{2}, \frac{1}{2}, \frac{3}{2})$  magnetic Bragg reflections measured with polarized neutrons (b). The vertical lines correspond to the two transition temperatures. The experimental and calculated integrated intensities for magnetic reflections using unpolarized neutrons at  $T = 11.5$  K (c) and 7 K (d).

characterization are described elsewhere. [1] The elastic neutron-scattering experiments using unpolarized neutrons were carried out on the thermal neutron triple-axis spectrometer TAS2 installed at the guide hall of JRR-3 at Japan Atomic Energy Agency. Energy of scattered neutrons was fixed to be 14.7 meV. The horizontal collimator sequences were guide-80'-S-80'-80' or guide-80'-S-80'-open. Polarized neutron scattering experiments were carried out on the thermal neutron triple-axis spectrometers TAS-1 installed at the beam hall of JRR-3. Heusler alloy (111) fixed to 14.7 meV was used as monochromator and analyzer. Flipping ratio of  $\sim 25$  was obtained on some nuclear Bragg peaks. The single crystal was mounted with the [111] and [011] axes in the horizontal scattering plane, while a vertical guide field was applied. Contamination from higher-order beams was effectively eliminated using PG filters.

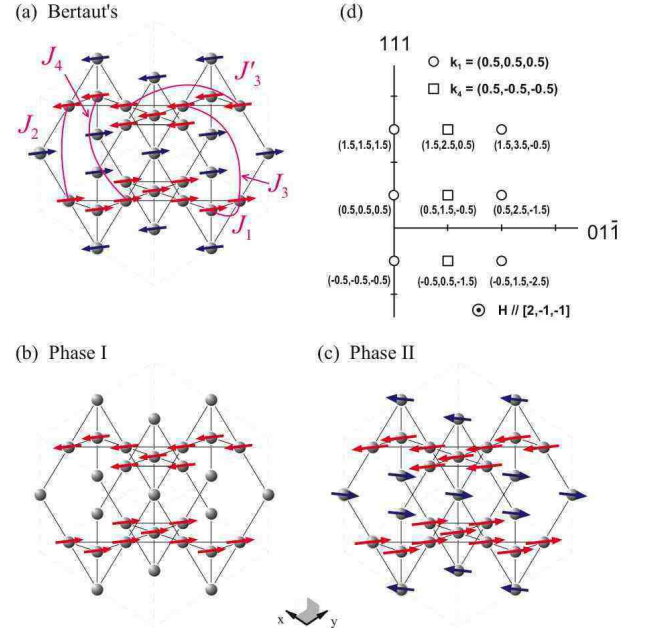


FIG. 2: (a) Bertaut's collinear spin model. (b) A collinear spin model for phase I with only kagome spins ordered. (c) A non-collinear spin model for phase II. All the spins are lying within the (1 1 1) plane, while the triangular and the kagome spins are pointing  $\sim 60^\circ$  away from each other. (d) The diagram of the horizontal scattering plane for the polarized neutron measurements. The circles and squares represent the magnetic Bragg reflections from the  $k_1$  and  $k_2$  domains, respectively. The guide field was applied perpendicular to the plane along  $[2\bar{1}\bar{1}]$ .

Bertaut *et al.* have performed neutron diffraction measurements [15] on a powder sample of  $\text{GeNi}_2\text{O}_4$  and showed that at 4 K spins are in a long-range ordered state with a characteristic wave vector of  $\mathbf{Q} = (1/2, 1/2, 1/2)$ . They have proposed as the ground state a collinear spin structure in which, as shown in Fig. 2 (a), the spins in kagome and triangular planes are aligned ferromagnetically in each plane and are stacked antiferromagnetically along the (111) direction. Our unpolarized elastic neutron scattering on a single crystal of  $\text{GeNi}_2\text{O}_4$  confirmed the characteristic wave vector being  $\mathbf{Q} = (1/2, 1/2, 1/2)$ . Figure 1(a) shows the temperature dependence of the magnetic Bragg intensities at  $\mathbf{Q} = (\frac{1}{2}, \frac{1}{2}, \frac{1}{2})$  and  $(\frac{1}{2}, \frac{1}{2}, \frac{3}{2})$ , obtained from the single crystal of  $\text{GeNi}_2\text{O}_4$ . Both data show a sharp increase in intensity around 12.1 K (phase I) with another sharp increase around 11.4 K (phase II), which indicates the existence of two distinct magnetic transitions and is consistent with the recent neutron powder diffraction data [2].

Our single crystal data, however, allow us to study the nature of the phase transitions in a more detail than the previous powder diffraction studies. The ratio of the intensities of the two reflections,  $I(\frac{1}{2}, \frac{1}{2}, \frac{1}{2})/I(\frac{1}{2}, \frac{1}{2}, \frac{3}{2})$ , changes as the system goes from phase I to phase II.

This indicates that the phases I and II have different spin structures. In order to investigate the ordered states in detail, we have performed unpolarized elastic scattering at nine independent magnetic Bragg reflections at 7 K (phase II) and 11.5 K (phase I). The scans were made along the longitudinal directions in the momentum space. Their integrated intensities are summarized in a log scale in Fig. 1 (c) and (d). The data were fitted to spin structures that are allowed by a linear combination of the basis vectors of irreducible representations for the  $Fd\bar{3}m$  group with  $\mathbf{Q} = (\frac{1}{2}, \frac{1}{2}, \frac{1}{2})$  [16, 17]. Since there is a 3-fold symmetry within either triangular or kagome planes, the calculated intensities were averaged among three equivalent spin orientations.

Interestingly, the collinear spin structure proposed by Bertaut *et al* (Fig. 2 (a)) [15] could not reproduce our phase I data. Furthermore, none of coplanar models where all spins lie on the same plane could fit our data, as long as both kagome and triangular spins are ordered [18] (see the pink line in Fig. 1 (c)). Instead, the data was best fitted to a spin structure with only the kagome spins ordered with  $\langle M \rangle_{kag}^I = 1.3\mu_B$  and with the triangular spins disordered (the black line in Fig. 1 (c)). This ordering of partial spins can be understood when we consider the internal magnetic field at the triangular sites due to the neighboring kagome spins. Since the triangular plane is sandwiched by two kagome planes below and above, the internal magnetic field due to the two kagome planes cancel each other on the triangular sites. Thus even when the system cools down and the kagome spins order, the triangular spins lying in between the kagome planes cannot order.

When the system cools further down to phase II, the relative intensities of the magnetic Bragg reflections change (Fig. 1 (d)), indicating that the spin structure is different from that of phase I. Since the unpolarized neutron scattering data are rather insensitive to the orientation of the weak triangular spins, the data can be reproduced equally well by several models: any coplanar models (see Fig. 2 (a) or (c)) with both the triangular and the kagome spins ordered within the  $\langle 111 \rangle$  plane with  $\langle M \rangle_{kag}^{II} = \langle M \rangle_{tri}^{II} = 1.8\mu_B$  (purple line in Fig. 1 (d)), to which the Bertaut's model belongs, and non-coplanar models where the triangular spins are aligned perpendicular to the  $\langle 111 \rangle$  plane whereas the kagome spins are in the plane. In the non-coplanar model, the best fit was obtained with the triangular spins having smaller moments,  $\langle M \rangle_{tri}^{II} = 1.3\mu_B$ , than the kagome spins,  $\langle M \rangle_{kag}^{II} = 2.0\mu_B$  (green line in Fig. 1 (d)), which is more or less what a recent powder diffraction study has proposed [19]. In any case, our unpolarized neutron scattering results clearly show for the first time that the two phase transitions in  $\text{GeNi}_2\text{O}_4$  are due to changes in the triangular layers, and it makes sense that these are harder to order since their interactions are more frustrated. Our finding also explains the origin of the two

distinct types of magnetic environment found in a recent muon-spin relaxation study [20].

Determining the actual spin directions uniquely using unpolarized neutron scattering data is difficult, if not impossible, because the intensities are usually insensitive to the orientation of the spins, as shown above. In order to distinguish the different models for the spin structure of phase II, we have performed polarized neutron measurements with a weak vertical guide field. The four possible  $\{111\}$  axes for ordering define four kinds of domains according to the angle between the ordering vector and the magnetic field:  $\mathbf{k}_1 = (1/2, 1/2, 1/2)$  with  $\theta_{H,Q} = 90^\circ$ ,  $\mathbf{k}_4 = (1/2, -1/2, -1/2)$  with  $\theta_{H,Q} = 19.5^\circ$ , and  $\mathbf{k}_2 = (-1/2, -1/2, 1/2)$ ,  $\mathbf{k}_3 = (-1/2, 1/2, -1/2)$  with the same intermediate angle. We selected a magnetic  $(1/2, 3/2, -1/2)$  Bragg peak that belongs to the  $\mathbf{k}_4$  domain, as the corresponding kagome planes are closely perpendicular to the neutron polarization direction ( $\sim 70.5^\circ$ ) and thus the scattering in the non-spin-flip (NSF) channel is mainly due to the spin components perpendicular to the kagome planes. (94 % of the out-of-plane components and 34 % of the inplane components contribute to the NSF scattering.) Fig. 1(b) shows the temperature dependence of the spin-flip (SF) and non-spin-flip (NSF) intensities of the reflection. The measured ratio of SF to NSF intensities is  $I_{\text{exp}}(\text{SF})/I_{\text{exp}}(\text{NSF}) = 8.7(8)$  after the correction for the imperfect polarization efficiency, and it stays almost constant. The measured ratio can be best reproduced when we assume all spins lie in the  $\langle 111 \rangle$  plane,  $I_{\text{cal}}(\text{SF})/I_{\text{cal}}(\text{NSF}) = 8.27$ , and the agreement rapidly worsens when the spins are allowed to have an out-of-plane component. So we conclude that in phase II both kagome and triangular layer spins lie in the  $\langle 111 \rangle$  plane with an unknown angle between them.

Can we interpret the ordering pattern in terms of exchange interactions? The first five of these involve one to two Ni - O - Ni or Ni - O - Ge superexchange steps [see Fig. 2 (a) and Table I]. The electronic configuration  $\text{Ni}^{2+}(e_g^2)$  and the Goodenough-Kanomori rules for these exchange paths imply that  $J_1$ ,  $J_2$ , and  $J_3$  should be weak, whereas  $J_3$  and  $J_4$  are comparably strong and antiferromagnetic (= positive in our convention); Note that, as there is no structural distortion, the spin layers form through a spontaneous symmetry breaking (in which one of the four  $\{\frac{1}{2}, \frac{1}{2}, \frac{1}{2}\}$  ordering vectors is arbitrarily chosen.) In fact, the "triangular" sites just consist of one of the four fcc sublattices of the pyrochlore structure, while the "kagome" sites are the union of the other three fcc sublattices.

We considered candidate states with collinear spins in which each sublattice might independently have ordering vector  $\mathbf{Q} = \{1, 0, 0\}$ ,  $\mathbf{Q} = \{1, 1, 0\}$ , or  $\mathbf{Q} = \{\frac{1}{2}, \frac{1}{2}, \frac{1}{2}\}$  (either aligned or not with that sublattice's unique  $\{111\}$  axis), focusing on spin arrangements competitive with the observed  $\mathbf{Q} = (\frac{1}{2}, \frac{1}{2}, \frac{1}{2})$  pattern, when  $J_3$ , and  $J_4$  are assumed strong and antiferromagnetic. In the observed

structure, the triangular and the kagome layers have different mean-field energies per spin:

$$E_{\text{kag}} = 2J_1 - J_3 + J'_3 - 4J_4; \quad (1a)$$

$$E_{\text{tri}} = 3J_3 - 3J'_3, \quad (1b)$$

obtained using the counts in Table I. This gives a net energy/spin  $E_{\text{tot}} = \frac{3}{4}E_{\text{kag}} + \frac{1}{4}E_{\text{tri}} = \frac{3}{2}J_1 - 3J_4$ . By comparison, structures built from  $Q = (100)$  or (110) would give  $E_{\text{tot}}^* = -J_3 - J'_3 + 3J_6 \pm |J_1 - 2J_2 + 2J_4|$ . Thus necessary condition to stabilize the actual structure is  $E_{\text{tot}} < E_{\text{tot}}^*$ , implying

$$J_4 > \frac{5}{2}J_1 - 2J_2 + J_3 + J'_3. \quad (2)$$

which is plausible for  $\text{GeNi}_2\text{O}_4$ . Note that when  $J_4$  dominates, the observed phase-I pattern of kagome layers with disordered triangular layers is the most stable mode in a mean-field approach.

As to the ordering temperatures, mean-field theory predicts  $k_B T_{N1} = \frac{2}{3}|E_{\text{kag}}|$  and  $k_B T_{N2} = \frac{2}{3}|E_{\text{tri}}|$ , so  $T_{N2} \lesssim T_{c1}$  implies [using (1a) and (1b)] that  $J_4 - J_1/2 \gtrsim J'_3 - J_3$ , which is consistent with the Goodenough-Kanamori rules. However, those rules would suggest  $E_{\text{tri}} \approx 3J_3 > 0$ , so it is surprising that  $T_{N2}$  is close to  $T_{N1}$ . Indeed, to ensure that the triangular spins order with the same  $Q = (\frac{1}{2}, \frac{1}{2}, \frac{1}{2})$  as the others (rather than the competing wavevectors), we must have  $J'_3 > J_3$ ;  $J'_3$  may be antiferromagnetic and  $J_3$  ferromagnetic.

A remaining question is, what causes *both* kagome and triangular spins to point within the plane of the layers? It cannot be the uniaxial anisotropy of each spin (with respect to its local three-fold axis): when averaged over the three sublattices forming the kagome spins, this must have a sign *opposite* to the anisotropy of the triangular spins. (since the anisotropy of all four sublattices averages to zero.) Nor can it be interlayer Dzyalohinski-Moriya (DM) couplings: these cancel by symmetry since the spins are ferromagnetic in each layer. The simplest explanation of the observed spin orientations is thus dipolar anisotropy. [Anisotropic exchange couplings will also generate an effective anisotropy for either kind of spin layer, the sign of which depends on details of the anisotropy and competition among the exchange interactions.]

In conclusion, our analysis suggests that in  $\text{GeNi}_2\text{O}_4$ ,  $J_4$  is the key interaction driving the first phase transition at  $T_{N1}$ . However, two discrepancies suggest our exchange-interaction model is incomplete in describing the triangular layer behavior: (i) the exchange theory

would actually predict helimagnetic order with  $Q = (\frac{1}{2} + \delta, \frac{1}{2} + \delta, \frac{1}{2} + \delta)$  (with  $|\delta| \gtrsim 0.01$ ), in analogy to a  $J_1$ - $J_2$  chain with  $J_2 \gg |J_1|$ ; contrary to observation in  $\text{GeNi}_2\text{O}_4$  (as well as related compounds). (ii) Exchange theory indicates FM  $J_3$  and AFM  $J'_3$ , which is unlikely by the Goodenough-Kanamori rules. A complete understanding may require models with anisotropic interactions or disorder, as well as spin-wave experiments to better constrain the  $\{J_i\}$ .

We would like to thank D. Khomskii and K. Kohn for stimulating discussions and Y. Shimojo for technical assistance. S.H.L. is supported by the U.S. DOE through DE-FG02-07ER45384, M.M. by MEXT of Japan and JSPS. and C.L.H. by NSF grant DMR-0552461.

- 
- [1] K. Matsuno *et al.*, unpublished (2002).
  - [2] M. K. Crawford *et al.*, Phys. Rev. B **68**, 220408(R) (2003).
  - [3] A. P. Ramirez, in *Handbook of Magnetic Materials*, edited K. J. H. Buschow (Elsevier, Amsterdam, 2001), Vol. 13.
  - [4] S. T. Bramwell and M. J. P. Gingras, Science **294**, 1495 (2001).
  - [5] R. Moessner and J. Chalker, Phys. Rev. Lett. **80**, 2929 (1998); Phys. Rev. B **58**, 12049 (1998).
  - [6] B. Canals and C. Lacroix, Phys. Rev. Lett. **80**, 2933 (1998); Phys. Rev. B **61**, 1149 (2000).
  - [7] U. Hizi and C. L. Henley, J. Phys. - Cond. Matt. **19** (14), 145268 (2007).
  - [8] S.-H. Lee *et al.*, Nature **418**, 856 (2002).
  - [9] S.-H. Lee *et al.*, Phys. Rev. Lett. **84**, 3718 (2000); S.-H. Lee *et al.*, J. Phys. - Cond. Matt. **19** (14), 145259 (2007).
  - [10] J.-H. Chung *et al.*, Phys. Rev. Lett. **95**, 247204 (2005).
  - [11] M. Matsuda *et al.*, Nature Physics **3**, 397 (2007).
  - [12] H. Tsunetsugu and Y. Motome, Phys. Rev. B **68**, 060405(R) (2003).
  - [13] S.-H. Lee *et al.*, Phys. Rev. Lett. **93**, 156407 (2004).
  - [14] Z. Zhang *et al.*, Phys. Rev. B **74**, 014108 (2006). 057204 (2002).
  - [15] E. F. Bertaut *et al.*, J. Phys. (France) **25**, 516 (1964).
  - [16] Yu. A. Izyumov, V. E. Naish, and R. P. Ozerov, *Neutron Diffraction of Magnetic Materials*, (Plenum Publishing Corporation, New York) 1991.
  - [17] J. D. M. Champion *et al.*, Phys. Rev. B **64**, 140407(R) (2001).
  - [18] Note that the observed intensities averaged among three  $S$ -domains are independent of the spin orientations within kagome planes.
  - [19] S. Diaz *et al.*, Phys. Rev. B **74**, 092404 (2006).
  - [20] T. Lancaster *et al.*, Phys. Rev. B **73**, 184436 (2006).
  - [21] Y. Yamada *et al.*, Phys. Rev. B **66**, 064401 (2002); K. Kamazawa *et al.*, Phys. Rev. B **70**, 024418 (2004).

TABLE I: List of the  $n$ th nearest-neighbor interactions in a spinel,  $\text{AB}_2\text{O}_4$ , up to  $n = 4$  and their possible *super*-exchange paths via anions (O) and A- or B-site transition metal ions.  $J$ ,  $d$ ,  $\theta$ ,  $n_B$ , and  $Z$  represent the coupling constant, the bond distance in a unit of  $a/4$ , the bond angle, the number of the exchange path, and the number of bonds, respectively. The symbol (I) stands for couplings being in  $\langle 111 \rangle$  planes, (K) and (T) for those with neighboring kagome and triangular layers, respectively.  $Z_K$  and  $Z_T$  are the number of bonds per a kagome and per a triangular spin, respectively. According to Goodenough-Kanamori rules, when B ions have  $e_g$  electrons, the superexchange *BOB* is sensitive to the bond angle: it can be ferromagnetic (for  $\theta \leq 96^\circ$ ) or antiferromagnetic (for  $\theta \geq 96^\circ$ ).

$J$	$d$	Path	$\theta$	$n_B$	$Z_K$	$Z_T$
$J_1$	$\sqrt{2}$	<i>BOB</i>	$90^\circ$	2	4 (I), 2 (T)	6 (K)
$J_2$	$\sqrt{6}$	<i>BOAOB</i>	$125^\circ, 125^\circ$	1	4 (I), 4 (K), 4 (T)	12 (K)
		<i>BOBOB</i>	$90^\circ, 90^\circ$	4		
$J_3$	$\sqrt{8}$	<i>BOAOB</i>	$125^\circ, 125^\circ$	2	2 (I), 4 (K)	6 (I)
$J'_3$	$\sqrt{8}$	<i>BOBOB</i>	$90^\circ, 90^\circ$	4	4 (I), 2 (K)	6 (T)
$J_4$	$\sqrt{10}$	<i>BOAOB</i>	$125^\circ, 125^\circ$	1	8 (K), 4 (T)	12 (K)